Journal Title
XX(X):1–12
©The Author(s) 2018
Reprints and permission:
sagepub.co.uk/journalsPermissions.nav
DOI: 10.1177/ToBeAssigned
www.sagepub.com/
SAGE

# Torque Vectoring based Drive Assistance System for Turning an Electric Narrow Tilting Vehicle

**Yaxing Ren[1], Truong Quang Dinh[2], James Marco[2], David Greenwood[2]**

### Abstract

The increasing number of cars leads traffic congestion and limits parking issue make in urban area. The narrow tilting vehicles (NTV) therefore can potentially become the next generation of city cars due to its narrow width. However, due to the difficulty in leaning an NTV, a drive assistance strategy is required to maintain its roll stability during a turn. This paper presents an effective approach using torque vectoring method to assist the rider in balancing the NTV and thus, reducing the counter-steering requirements. The proposed approach is designed as the combination of two torque controllers, steer angle based torque vectoring (SATV) controller and tilting compensator based torque vectoring (TCTV) controller. The SATV controller is to reduce the counter-steering process via adjusting the vectoring torque based on the steering angle from rider. Meanwhile the TCTV controller develops the SATV with an additional tilting compensator to help balancing the leaning behaviour of NTVs. Numerical simulations with a number of case studies have been carried out to verify the performance of designed controllers. The results imply that the counter-steering process can be eliminated and the roll stability performance can be improved with the usage of the presented approach.

### Keywords

Roll stability, torque vectoring, drive assistance, narrow tilting vehicle

## Introduction

Considering the practical dimensions and low energy consumption, electric vehicles are expected to be the main transportation in a near future. The increasing number of cars leads the problems of traffic congestion and limit parking places make in urban area. Due to this issue, small narrow commuter vehicles are required to become a new generation of city cars (Ren, et al. (2018)), as the two prototype vehicles developed in the RESOLVE project shown in Figure 1. The narrow commuter vehicles have four wheels as a car but with just half the width of a conventional car, like a motorcycle. This makes a narrow commuter vehicle integrate the features and advantages of a car and a motorcycle, but causes its roll stability an issue (Ruggero and Alessandro (2006); Fabien, et al. (2014); Pojani and Stead (2015); Li, et al. (2017)).

In order to maintain lateral stability, the narrow commuter vehicles should have to lean into corners during turning like two-wheeled vehicles (Van (2011); Fajans (2000)). This kind of vehicles are also called narrow tilting vehicles (NTVs). Different with the conventional vehicles that have roll stiffness to balance the roll stability by it own suspension structure, the NTV has no such roll stiffness. Thus, the NTVs are easy to fall down during a turn if its roll stability cannot be well maintained. This is the main challenge in NTVs.

Unlike the case of a motorcycle that the rider can shift his weight to lean the motorcycle into a corner, the mass of a NTV is much higher than that of a human body (Van (2011)). The rider has to act on the counter-steering and throttle to balance the vehicle in a turn (Fajans (2000); Van (2011)). In normal steering method, a rider has to manage the following actions:

1) To provide a counter steering on the throttle;


**Figure 1.** Two demonstrators of narrow tilting vehicle developed in the RESOLVE project (RESOLVE (2018)).

2) To provide the lateral force causing a yaw rate to the opposite direction and a roll rate to the desired direction;

3) To turn the steering to the desired direction shortly after the counter-steering;

4) To create the vehicle yawing to the desired direction.

[1]School of Engineering, University of Glasgow, Glasgow, G12 8QQ, UK
[2]Warwick Manufacturing Group (WMG), University of Warwick, Coventry, CV4 7AL, UK

**Corresponding author:**
Yaxing Ren, School of Engineering, University of Glasgow, Glasgow, G12 8QQ, UK.
Email: yaxing.ren@glasgow.ac.uk

It shows that the riders of NTVs are required to be very experienced in controlling the vehicle in balancing and path-following. However, the next generation vehicle should be much easier to be ridden by any kinds of riders, from new to experienced. Therefore, it is required to develop an assistance system for the rider in tilting and balancing the NTV.

From literature, the common solution to solve this issue is to use external mechanisms for the active tilting control. The two main tilting methods are the steering tilt control (STC) and the direct tilt control (DTC) (Mourad, Claveau and Chevrel (2014); Snell (1998)), one aims to control directly on the steering angle and the other aims to provide addition moment of torque to tilt the vehicle. As studied in previous researches, the STC system is efficient at high speed but the balancing does not suit well at the standstill or very low speeds and perform even worse in slippery road conditions (Van, Brink and Kroonen (2004)). The DTC system simplifies the control with an additional tilt actuator but it requires high tilting motion and the delayed actuator response causes the risk of vehicle oscillations (Kidane, et al. (2008)). Both of the approaches are requiring additional mechanisms to adjust the performance of vehicle following rider's behaviour. This paper presents an alternative way of using torque vectoring (TV) techniques to assist the rider in balancing the NTV and simplify the steering process of turning the NTV without any additional mechanisms, as shown in Figure 2.

The traditional TV technology can improve the vehicle cornering response and it has the potential to improve the handling response of a vehicle (Leonardo, et al. (2014)). The first left-right TV technique has been proposed in (Sawase and Sano (1999)) aims to distributing driving and braking forces acting upon the right and left wheels in a wheel-individual vehicle (Koehler, et al. (2017)). The different mechanisms and control allocation criteria have been reviewed and compared for their performances and sensitivities to electric motor drive parameters in (Sawase, Ushiroda and Miura (2006); Sawase and Ushiroda (2008); Leonardo, et al. (2014)). The maximum vectoring torque limit has been determined in (Sawase and Ushiroda (2008)) and desired traction force and yaw moment input has been mapped in (Kang, et al. (2012)) using an optimal TV algorithm. In recent literature, the TV approach has been optimized to improve the yaw moment distraction performance (Yim, Choi and Yi (2012)), improve its stability under expected road and driving conditions (Fallah, et al. (2013)), maximize the driving velocity and enhance the lateral stability in cornering on (Her, et al. (2016)), and minimize the power losses on a battery electric vehicle (Koehler, et al. (2017)). In these approaches, the TV method is used as assistant torque for vehicle yaw turn in normal vehicles as its roll stability is not a main issue. However, the roll stability maintenance needs to be paid more attention in an NTV and the conventional TV method is not suitable to be used in this types of vehicles. In this point of view, none of the previously designed torque controllers has considered the feature of NTV to assist the rider in balancing the vehicle in a turn of using TV technology.

This paper aims to develop and implement the TV technology to assist the rider to maintain the roll dynamics of NTV in cornering. The proposed approach is designed as the combination of two torque controllers, steer angle based torque vectoring (SATV) controller and tilting compensator based torque vectoring (TCTV) controller. The SATV controller is to manage the vectoring torque based on the steer angle in order to reduce the counter-steering process, while the TCTV controller use a further tilting compensator to improve the tilting stability of NTVs. The developed TV controllers have the ability to reduce the counter-steering requirements from rider and improve the tilting behaviour during turning an NTV. As a result, both the new rider and experienced rider can drive the NTV easily.

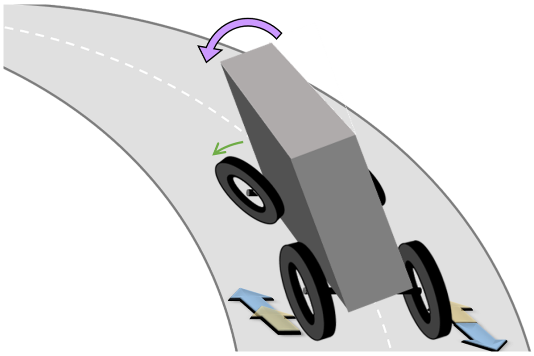

**Figure 2.** Vectoring torque assists the rider in balancing the NTV during a turn.

## Mathematical Model of Four-Wheel Vehicle Dynamics

### *Wheel Dynamics*

In the rear-wheel-drive vehicles, the wheel speed $\omega_{ij}$ are presented to describe the power transfer from wheel hub to road as follows Li, et al. (2017); Kumar, et al. (2014):

$$\dot{\omega}_{\mathrm{f}j} = \frac{-T_{\mathrm{brk,f}} - R_{\mathrm{f}} F_{\mathrm{l,f}j}}{J_{\mathrm{f}j}} \tag{1}$$

$$\dot{\omega}_{\mathrm{r}j} = \frac{T_{\mathrm{r}j} - T_{\mathrm{brk,r}} - R_{\mathrm{r}} F_{\mathrm{l,r}j}}{J_{\mathrm{r}j}} \tag{2}$$

where $J_{ij}$ is the wheels' inertia around the wheel with the radius $R_i$ with $ij \in \{\text{fl,fr,rl,rr}\}$ that represent the front left, front right, rear left, and rear right wheel, respectively. The wheels are driven by the torque $T_{\mathrm{r}j}$ that applied on the left and right rear wheels that resistant by the brake torque $T_{\mathrm{brk},i}$ and longitudinal force $F_{\mathrm{l},ij}$ at the contact point between road and tyre. The longitudinal force can be described as a function of friction coefficient $\mu_{ij}$ and tyre longitudinal slip $s_{\mathrm{l},ij}$ as

$$F_{\mathrm{l},ij} = F_{\mathrm{z},ij} \cdot \mu_{ij}\left(s_{\mathrm{l},ij}\right) \tag{3}$$

The tyre characteristics are modeled by the *magic tyre formula* in the research of Pacejka (2005) as

$$\mu_{ij}\left(x_{ij}\right) = \sin\left\{C \arctan\left[B(1-E)\cdot x_{ij} + E\arctan(B\cdot x_{ij})\right]\right\} \tag{4}$$

where $B$, $C$, $E$ are tyre parameters determined by measurements, $x_{ij}$ can be the longitudinal slip $s_{\mathrm{l},ij}$ or lateral slip angle $\alpha_{ij}$ to calculate the longitudinal slip force or side slip force Svendenius (2007). $F_{z,ij}$ is the vertical load of each wheel that can be calculated by

$$F_{z,fl} = m\left(\frac{l_r}{l}g - \frac{h}{l}a_x\right)\left(\frac{1}{2} - \frac{h}{b_f}\frac{a_y}{g}\right) \quad (5)$$

$$F_{z,fr} = m\left(\frac{l_r}{l}g - \frac{h}{l}a_x\right)\left(\frac{1}{2} + \frac{h}{b_f}\frac{a_y}{g}\right) \quad (6)$$

$$F_{z,rl} = m\left(\frac{l_f}{l}g + \frac{h}{l}a_x\right)\left(\frac{1}{2} - \frac{h}{b_r}\frac{a_y}{g}\right) \quad (7)$$

$$F_{z,rr} = m\left(\frac{l_f}{l}g + \frac{h}{l}a_x\right)\left(\frac{1}{2} + \frac{h}{b_r}\frac{a_y}{g}\right) \quad (8)$$

where $m$ is the vehicle mass; $l$ is the wheelbases which consists the distance from the center of gravity (COG) to the front and rear axles as $l_f$ and $l_r$; $h$ is the height of vehicle COG from the road surface; $b_f$ and $b_r$ are the track of front and rear axle;and $g$ is the gravitational constant. $a_x$ and $a_y$ are the vehicle acceleration in $x$ and $y$ axis.

And tyre longitudinal slip $s_{l,ij}$ can be described based on the vehicle velocity $v$ and vehicle side-slip angle $\beta$ as:

$$s_{l,ij} = \frac{R_i\omega_{ij} - v\cos\beta}{\max(R_i\omega_{ij}, v\cos\beta)} \quad (9)$$

The sideslip force of tyre is also represented with the magic tyre formula in (4) as

$$F_{s,ij} = F_{z,ij}\cdot[\mu_{ij}(\alpha_{ij}) + \lambda_{st}\theta] \quad (10)$$

where $\lambda_{st}$ is the camber stiffness coefficient of tyre and $\theta$ is the roll angle of tilting vehicle. The lateral slip angle of front and rear wheels $\alpha_{ij}$ is the angle between the wheels' velocity vector and its longitudinal axis, which can be can be calculated by

$$\alpha_{fj} = \delta - \arctan\left(\frac{v\sin\beta + l_f\dot{\varphi}}{v\cos\beta}\right) \quad (11)$$

$$\alpha_{rj} = -\arctan\left(\frac{v\sin\beta - l_r\dot{\varphi}}{v\cos\beta}\right) \quad (12)$$

where $\delta$ is the steering angle of front wheels, and $\dot{\varphi}$ is the yaw rate of thte vehicle.

To present the forces in the vehicle-fixed coordinate system, the traction force of front wheels $F_{x,fj}$ and lateral force of front wheels $F_{y,fj}$ are given by the transformation

$$F_{x,fj} = F_{l,fj}\cos\delta - F_{s,fj}\sin\delta \quad (13)$$

$$F_{y,fj} = F_{l,fj}\sin\delta + F_{s,fj}\cos\delta \quad (14)$$

and the traction and lateral force of rear wheels $F_{x,rj}$ and $F_{y,rj}$ are calculated equal to the longitudinal and side-slip force $F_{l,rj}$ and $F_{s,rj}$, respectively.

### *Vehicle Dynamics*

The vehicle model of narrow tilting vehicle includes the velocity dynamic, side-slip angle dynamic, yaw dynamic and roll dynamic (Koehler, et al. (2017)). The geometry model of a NTV is shown as in Figure 3. The vehicle motion dynamics can be described by the vehicle velocity $v$ and the vehicle side-slip angle $\beta$, which is defined as the angle between $v$ and the vehicle longitudinal axis $x$. Their dynamics can be represented by the differential equations

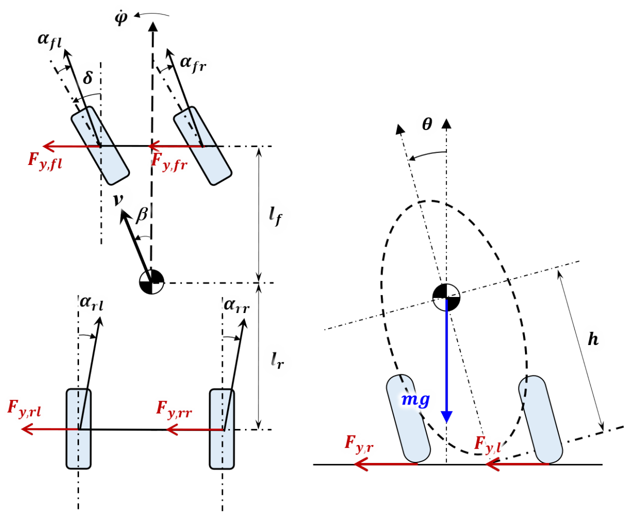


**Figure 3.** Geometry of a narrow tilting vehicle.

$$\dot{v} = \frac{1}{m}\left(\cos\beta\sum_{ij}F_{x,ij} + \sin\beta\sum_{ij}F_{y,ij} - F_{res}\right) \quad (15)$$

$$\dot{\beta} = \frac{1}{mv}\left(\cos\beta\sum_{ij}F_{y,ij} - \sin\beta\sum_{ij}F_{x,ij}\right) - \dot{\varphi} \quad (16)$$

where $F_{res}$ represents the force of driving resistance.

The vehicle acceleration can be calculated with the relationship of $v$, $\beta$, $\varphi$ and their differentials as

$$a_x = \dot{v}\cos\beta - v(\dot{\beta} + \dot{\varphi})\sin\beta \quad (17)$$

$$a_y = \dot{v}\sin\beta + v(\dot{\beta} + \dot{\varphi})\cos\beta \quad (18)$$

The yaw motion of the vehicle can be calculated as the differential equation

$$\ddot{\varphi} = \frac{1}{I_z}\Big[l_f(F_{y,fl} + F_{y,fr}) - l_r(F_{y,rl} + F_{y,rr}) + \frac{b_f}{2}(F_{x,fr} - F_{x,fl}) + \frac{b_r}{2}(F_{x,rr} - F_{x,rl})\Big] \quad (19)$$

where $I_z$ is the inertia moment about the vertical axis.

Differently with the roll damping dynamic of normal vehicles, the NTV has no roll stiffness of suspension. Thus, it is not self-stable in the roll motion and could finally fall down. The equation of roll motion of NTV is described as

$$\ddot{\theta} = \frac{1}{I_x + mh^2\sin^2\theta}\Big[mhg\sin\theta - h\cos\theta\sum F_{y,ij} - mh^2\dot{\theta}^2\sin\theta\cos\theta - C_d\dot{\theta}\Big] \quad (20)$$

where $\theta$ and $\dot{\theta}$ are the vehicle roll angle and roll rate, $I_x$ is the vehicle roll moment of inertia, and $C_d$ is the roll damping ratio of the suspension.

## Torque Vectoring Control System Design

### *Simplified Single-track Vehicle Model*

The nonlinear equations of the four-wheel model provided in previous section are much more accurate in matching the real vehicle response. However, the complex nonlinear equations and the interactions between states are difficult to be used in controller design and performance analysis. Therefore, a simplified single-track model has been delivered from the nonlinear equations (1) to (20). To simplified the model, it is assumed that the steer angle, side slip angle and roll angle are small and equaling to their sinusoidal value, the COG is at the middle of the vehicle track ($l_\mathrm{f} = l_\mathrm{r}$), and define the rear wheel torque differential value $\Delta T_\mathrm{r}$ as an additional system input. Then the vehicle model can be represented as a function of the system space vector $x$ and control vector $u$ as

$$\dot{x} = f(x) + g(x) \cdot u \tag{21}$$

where

$$x = \begin{bmatrix} v & \beta & \dot{\varphi} & \theta & \dot{\theta} \end{bmatrix}^T, \quad u = \begin{bmatrix} \delta & T_\mathrm{r} & \Delta T_\mathrm{r} \end{bmatrix}^T \tag{22}$$

$$f(x) = \begin{bmatrix} -\dfrac{2C_\gamma}{m}\beta^2 + \dfrac{2\lambda_\gamma}{m}\beta\theta \\ -\dfrac{2C_\gamma}{m}\dfrac{\beta}{v} + \dfrac{2\lambda_\gamma}{m}\dfrac{\theta}{v} - \dot{\varphi} \\ -\dfrac{C_\gamma l^2}{2I_\mathrm{z}}\dfrac{\dot{\varphi}}{v} \\ \dot{\theta} \\ \dfrac{mgh - 2\lambda_\gamma h}{I_\mathrm{x}}\theta - \dfrac{C_\mathrm{d}}{I_\mathrm{x}}\dot{\theta} + \dfrac{2C_\gamma h}{I_\mathrm{x}}\beta - \dfrac{mh^2}{I_\mathrm{x}}\dot{\theta}^2\theta \end{bmatrix} \tag{23}$$

$$g(x) = \begin{bmatrix} \dfrac{C_\gamma}{m}\beta & \dfrac{1}{mR_\mathrm{r}} & 0 \\ \dfrac{C_\gamma}{mv} & -\dfrac{\beta}{mv} & 0 \\ \dfrac{C_\gamma l}{2I_\mathrm{z}}\beta & 0 & \dfrac{b_\mathrm{r}}{I_\mathrm{z}} \\ 0 & 0 & 0 \\ -\dfrac{C_\gamma h}{I_\mathrm{x}} & 0 & 0 \end{bmatrix} \tag{24}$$

including the linearized tire lateral behaviour as equivalent cornering stiffness coefficient $C_\gamma$ and camber stiffness coefficient $\lambda_\gamma$.

The system will finally converge to its steady state with a given trajectory by assuming the deviation of system states are all zero. When the vehicle is turning in a circle with radius of $R$, the system steady state value of sideslip angle, yaw rate and roll angle can be approximately calculated as

$$\begin{cases} \beta_0 = l/2R \\ \dot{\varphi}_0 = v/R \\ \theta_0 = v^2/gR \end{cases} \tag{25}$$

## Virtual Rider Model

### A. Steering Control

This rider robot had two control aims: maintain standing stability and follow a target course (Van (2011)). In turning a NTV, the rider has to act on the counter-steering and throttle to balance the NTV in a turn. The NTV stability control algorithm needs to be developed considering as the rider has no special operating skills (Kidane, et al. (2006, 2008, 2010)). One solution is to apply two separate control algorithms, one to maintain the roll angle and the other to follow the path, and then put together the two systems to form the control algorithm for NTV.

In rider's roll stability control, a proportional derivative (PD) control algorithm was applied to maintain the roll angle (Van (2011)) as represented

$$\delta_1 = (k_\mathrm{p2} + sk_\mathrm{d2})(\theta_\mathrm{ref} - \theta) \tag{26}$$

In rider's lateral control, the rider implements on steering input to follow a certain desired lateral trajectory without regard to vehicle tilt stability, where the relationship between the path and steering angle is assumed to be linear (Van (2011)). The transient response of the lateral trajectory tracking is not urgent comparing with the roll stability control. Due to this, a pseudo-derivative feedback (PDF) control algorithm is applied to reduce the effect of derivative feed-forward action comparing with a traditional PI(D) control (Ohm (1994)). The lateral control of virtual rider that presents the steering angle for lateral trajectory tracking can then be designed as:

$$\delta_2 = \frac{k_\mathrm{i1}}{s}(\dot{\varphi}_\mathrm{ref} - \dot{\varphi}) - k_\mathrm{p1}\dot{\varphi} \tag{27}$$

Then the two systems will be combined together in the virtual rider model.

$$\delta = \delta_1 + \delta_2 \tag{28}$$

### B. Speed Control

Apart from the steering control to follow the path and maintain the roll stability, the rider also have to control the vehicle speed via throttle. The sensor installed in throttle send the position information to the controller to indicate the rider's torque demand. Then a torque reference is sent to the inverter control unit to drive the wheel motors. To simplify this process, the speed control is presented via a PI controller as the rider aims to track the target vehicle velocity.

$$T_\mathrm{r} = \left(k_\mathrm{p3} + \frac{k_\mathrm{i3}}{s}\right)(V_\mathrm{ref} - v) \tag{29}$$

## Torque Controller

### A. Steering Angle based Torque Vectoring (SATV)

To compensate the counter steering behaviour, the most easy way is to set the vectoring torque proportional to the derivative of steer angle as:

$$\Delta T_\mathrm{r} = K\dot{\delta} \tag{30}$$

where $K$ is the control gain to be adjusted for an expected controller performance. This control parameter is chosen to set the bandwidth of the torque vectoring controller in such a way that its speed of response faster than that of the vehicle yaw moment and slower than that of the wheel motor torque. A simple iteration loop can be utilised to enhance this task.

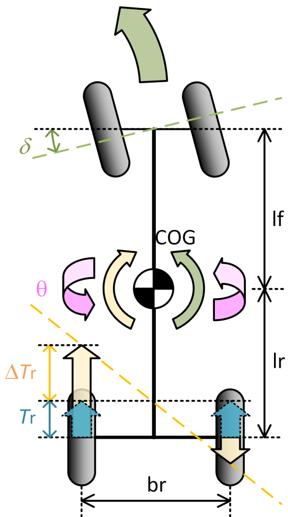


**Figure 4.** The diagram of torque vectoring for narrow tilting vehicle.

When the rider is willing to turn, the vectoring torque activated to make the vehicle yaw to the opposite direction and roll to the same direction as rider wishes until reached the steady state.

### *B. Tilting Compensator based Torque Vectoring (TCTV)*

After the virtual rider controls the vehicle yaw rate, the $\dot{\varphi}$ equals to the desired and $\ddot{\varphi}$ is assumed equal to zero. Then from the yaw dynamics in (21), the steady-state steer angle can be presented as:

$$\delta_{\mathrm{ss}} = \frac{l}{v}\dot{\varphi} - \frac{2b_{\mathrm{r}}}{C_\gamma l}\Delta T_{\mathrm{r}} \tag{31}$$

Substitute (31) into the roll dynamic equation in (21) to obtained a rewritted presentation as:

$$\begin{aligned}\ddot{\theta} = \quad & \frac{1}{I_{\mathrm{x}}}\Big[(mgh - 2\lambda_\gamma h)\theta - C_{\mathrm{d}}\dot{\theta} + 2C_\gamma h\beta - mh^2\dot{\theta}^2\theta \\ & -C_\gamma h\left(\frac{l}{v}\dot{\varphi} - \frac{2b_{\mathrm{r}}}{C_\gamma l}\Delta T_{\mathrm{r}}\right)\Big]\end{aligned} \tag{32}$$

Assume $\dot{\theta}$ and $\ddot{\theta}$ are zero in steady state, one can obtain the equation below:

$$\ddot{\theta} = \frac{h}{I_{\mathrm{x}}}\left[(mg - 2\lambda_\gamma)\,\theta + 2C_\gamma\beta - \frac{C_\gamma l}{v}\dot{\varphi} + \frac{2b_{\mathrm{r}}}{l}\Delta T_{\mathrm{r}}\right] = \sigma \tag{33}$$

If design the control signal as

$$\sigma = \frac{h}{I_{\mathrm{x}}}\frac{2b_{\mathrm{r}}}{l}K\dot{\delta} = K'\dot{\delta} \tag{34}$$

the vectoring torque for roll stability improvement can be delivered from (33) as

$$\Delta T_{\mathrm{r}} = K\dot{\delta} + \Psi \tag{35}$$

where

$$\Psi = \frac{l}{2b_{\mathrm{r}}}\left[C_\gamma\delta - (mg - 2\lambda_\gamma)\,\theta - 2C_\gamma\beta\right] \tag{36}$$

Comparing (35) with (30), one can find that there is an additional component $\Psi$, which is defined as the tilting compensator (TC). The TC based torque vectoring (TCTV) method can manage the vectoring torque to reduce the counter steering during a turn. The block diagram of the TV based drive assistance system is shown in Figure 5.

### *C. Torque Management*

As the main source of pure electric vehicles, the batteries perform significant roles in vehicle propulsion. Considering the limit output power of battery and electric motors, the torque controller should adjust the output torque to protect the equipment from over-current. The available torque can be represented as

$$T_{\mathrm{avi}} = \min\left(T_{\mathrm{m,rated}}, \frac{\min\left(P_{\mathrm{m,rated}}, P_{\mathrm{b,avi}}\right)}{\omega_m}\right) \tag{37}$$

where $T_{\mathrm{m,rated}}$ and $P_{\mathrm{m,rated}}$ is the rated torque and power of wheel motor from manufacturer; $P_{\mathrm{b,avi}}$ is the maximum output power from vehicle battery management system (BMS) based on the charging status of battery. Then the torque output is managed considering the available torque as

$$T'_{\mathrm{r}} = \min\left(T_{\mathrm{r}},\ T_{\mathrm{avi}}\right) \tag{38}$$

$$\Delta T'_{\mathrm{r}} = \min\left[\Delta T_{\mathrm{r}},\ (T_{\mathrm{avi}} - T'_{\mathrm{r}})\right] \tag{39}$$

Then the final torque applied on the left and right rear wheels can be represented as

$$\begin{cases} T_{\mathrm{rl}} = T'_{\mathrm{r}} + \Delta T'_{\mathrm{r}} \\ T_{\mathrm{rr}} = T'_{\mathrm{r}} - \Delta T'_{\mathrm{r}} \end{cases} \tag{40}$$

The torque drive system of NTV is shown in Figure 6, where the data flow, electric power flow, and mechanical drive are given with blue, red and black arrows, respectively.

### *D. Control objectives and stability analysis*

This paper focuses on the suppression of the roll motion. For the narrow tilting vehicle (NTV), the roll motion is the most significant index as the lack of roll stability will make the NTV easy to fall down when turns into a corner. The yaw motion will not affect the stability of vehicle and it aims to track the desired route which is not the primary control objective. In addition, the virtual rider in the closed-loop system aims to track the yaw rate. This can make the performance of yaw rate and sideslip angle of vehicle easy be adjusted by the operation of virtual rider and not considered in the proposed torque controller. Thus, the control objective of the drive assistance system is to suppression the roll rate to zero in finite time in the presence of unpredictable operation (the steer angle $\delta$) from rider.

The Bode plots of closed-loop system are shown in Figure 7 and 8 for SATV and TCTV based systems, respectively. In the Bode diagram, when the magnitude in dB below zero, the phase is greater than -180 $deg$ in all circumstances. It shows the closed-loop system will not amplify the system error and has ability to eliminate the error with damping applied on the closed-loop system. Comparing the Bode figures of SATV and TCTV, the TCTV based closed-loop system has better damping within the range of frequency between 0.8 $rad/s$ to 40 $rad/s$ (approximate 0.1 $Hz$ to 6 $Hz$), which covers the basic response speed of vehicle and rider. In normal

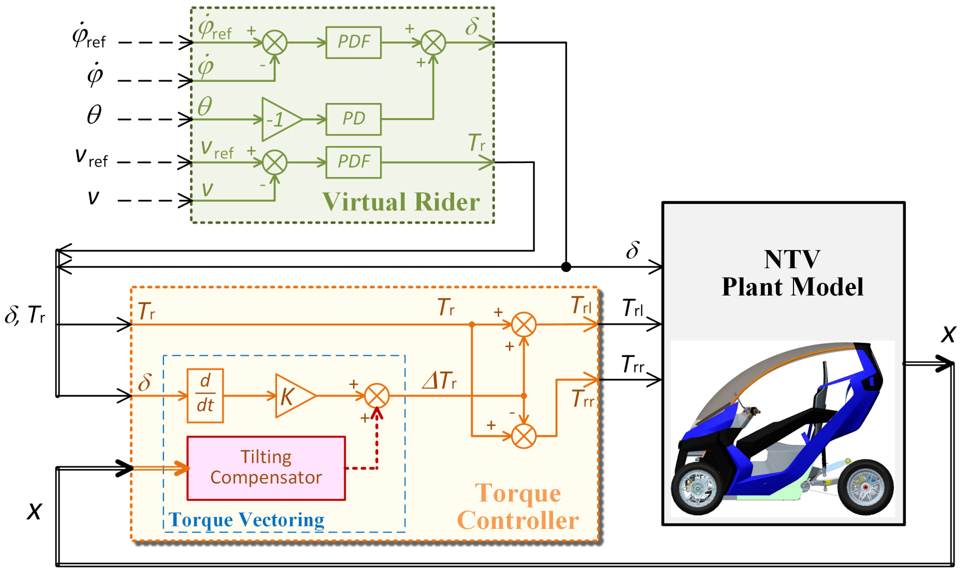


**Figure 5.** The control block diagram of torque vectoring.

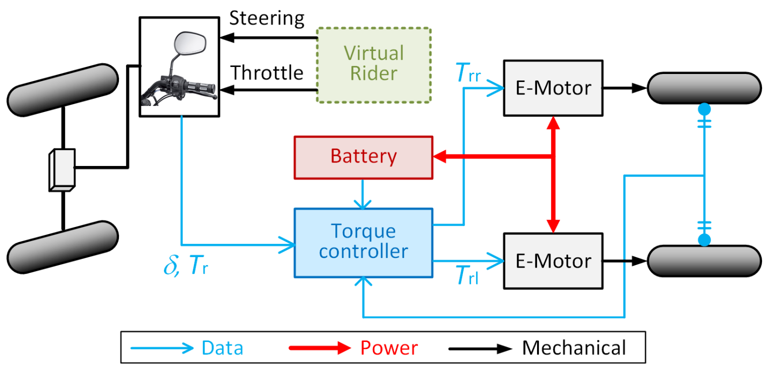


**Figure 6.** The diagram of torque vectoring for narrow tilting vehicle.

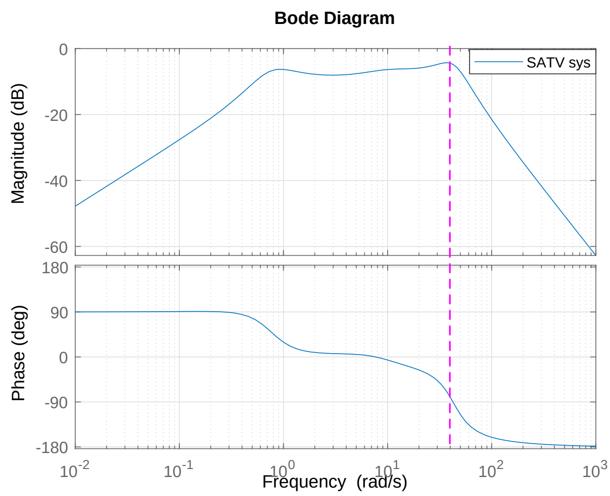


**Figure 7.** Bode diagram of SATV-based closed-loop system.

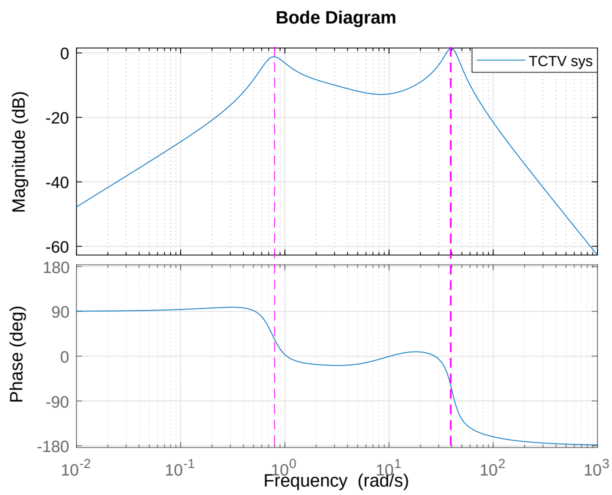


**Figure 8.** Bode diagram of TCTV-based closed-loop system.

driving cases, the closed-loop system performs better using the TCTV torque controller. The NTV system with both torque vectoring approaches is proved to be stable from low to high frequency.

**Table 1.** System parameters of NTV

| Description | Symbol | Value | Unit |
|---|---|---|---|
| Total vehicle mass | $m$ | 200.0 | kg |
| Height of vehicle COG | $h$ | 0.5 | m |
| Gravitational constant | $g$ | 9.81 | $\mathrm{m/s^2}$ |
| Distance from COG to front axle | $l_\mathrm{f}$ | 0.7 | m |
| Distance from COG to rear axle | $l_\mathrm{r}$ | 0.9 | m |
| Length of track of rear axle | $b_\mathrm{r}$ | 0.7 | m |
| Vehicle roll moment inertia | $I_\mathrm{x}$ | 18 | $\mathrm{kg{\cdot}m^2}$ |
| Vehicle yaw moment inertia | $I_\mathrm{z}$ | 80 | $\mathrm{kg{\cdot}m^2}$ |
| Front/Rear wheel radius | $R_{\mathrm{fj/rj}}$ | 0.5 | m |
| Front/Rear wheel rotational inertia | $J_{\mathrm{fj/rj}}$ | 0.2 | $\mathrm{kg{\cdot}m^2}$ |
| Front cornering stiffness | $C_\mathrm{f}$ | 3500 | N/rad |
| Rear cornering stiffness | $C_\mathrm{r}$ | 5480 | N/rad |
| Front camber stiffness | $\lambda_\mathrm{f}$ | 1000 | N/rad |
| Rear camber stiffness | $\lambda_\mathrm{r}$ | 2000 | N/rad |

**Table 2.** Controller parameter settings

| Description | Symbol & Value |
|---|---|
| Virtual rider | $k_{\mathrm{p1}} = 0.3$; $k_{\mathrm{i1}} = 0.2$<br>$k_{\mathrm{p2}} = 1$; $k_{\mathrm{d2}} = 5$<br>$k_{\mathrm{p3}} = 1$; $k_{\mathrm{i3}} = 0.4$ |
| Torque controller | $K = 50$<br>$T_{\mathrm{m,rated}} = 50$ Nm<br>$P_{\mathrm{m,rated}} = 1500$ W |

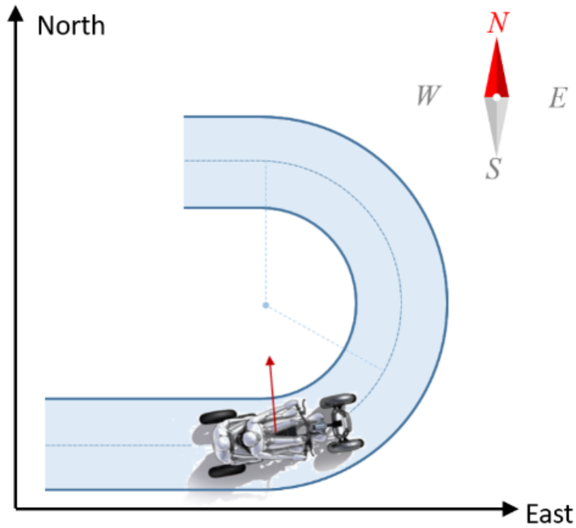


**Figure 9.** Path of vehicle with left turn in simulation.

## Simulation Results

The NTV parameters used for the simulation are from (Gohl (2006)) given in Table 1. The simulation validations are carried out with tracking the route of a step yaw rate in two case studies. The first case is that the vehicle driven into a turn at a constant speed and the second case is that the vehicle accelerating during a turn. For a fire comparison among different torque controllers of SATV controller, TCTV controller and the traditional controller without TV technology, all the tests use the same rider model and vehicle plant model. The parameter settings of the virtual rider model and torque controller are given in Table 2.

Due to the requirements of counter-steering process, it is a challenge for new riders to balance the vehicle and follow the path simultaneously when driving an NTV. Two simulation cases are designed to verify the control performances. The first case is chosen as driving into a turn to the left under a constant speed. With a step change on the steering reference, the torque controller will assist the rider to tilt the vehicle. The performance will validate the effectiveness of the designed controller on counter steering reduction. The second case is chosen as accelerating during a left turn. Accelerating or decelerating in a turn has the risk to cause the vehicle unstable. Thus, this operating case is chosen to verify the stability improvements of the designed controller.

### *Left Turn under Constant Speed*

The case study is to simulate the dynamic response of an NTV to start a turn in simulation. The vehicle is driven forward under a constant speed of 5 $m/s$ as an initial state. Then the rider starts to turn the vehicle to track the path of a circle with the radius of 15 $m$, as shown in Figure 9. The desired command to the virtual rider is a step change of yaw rate to achieve a perfect path follow. However, as the vehicle itself has its own yaw inertia and also roll inertia, it is not possible to reach the target yaw rate immediately. Thus, the step change of yaw rate reference actually acts as a sudden disturbance to the torque controller to verify its transient response. In conventional roll and yaw control method, the rider should counter-steer the front wheels to lean the vehicle into an opposite direction until the roll angle achieves the desired value to maintain its roll stability. Then the rider steer the front wheels to yaw the vehicle into the target direction for path following. All these reactions have to be completed within seconds. With the assist of torque vectoring, the requirements of counter-steer from rider will be reduced as the roll stability can be maintained via the torque controller through torque vectoring technology.

Figure 10 shows the dynamic response of the two inputs, the steering angle and vectoring torque, as well as the system states of vehicle side-slip angle, yaw rate, lateral acceleration, and roll rate. The comparisons are among the steering and torque control by rider, the traditional TV approaches, the SATV and TCTV based torque control to assist the same rider from the virtual model. In the steering angle comparison, both the SATV and TCTV based torque control methods have reduced the requirements of counter-steering from rider. The traditional TV approaches focused on the yaw moment of the vehicle to provide a steady-state torque when the vehicle is turning, while the proposed SATV and TCTV provide a transient torque when the vehicle starts to turn. In the vectoring torque comparison, the TCTV has less oscillation comparing with the SATV due to the compensation of tilting dynamics. In the system states, the vehicle velocity and roll angle of all the four controllers have no obvious difference. The steady state target value of the yaw rate can be calculated from (25) is 19 $deg/s$. The yaw rate and lateral acceleration of the TCTV based torque control have less oscillation comparing with the other three methods. The steady state target value of the side-slip angle is 2.9 $deg$. The performance of side-slip angle is significantly caused by steering angle so it has the same response of that of steering angle. The roll rate of the TCTV based torque control has the best performance with less peak roll rate and less oscillation. The SATV based torque control has better

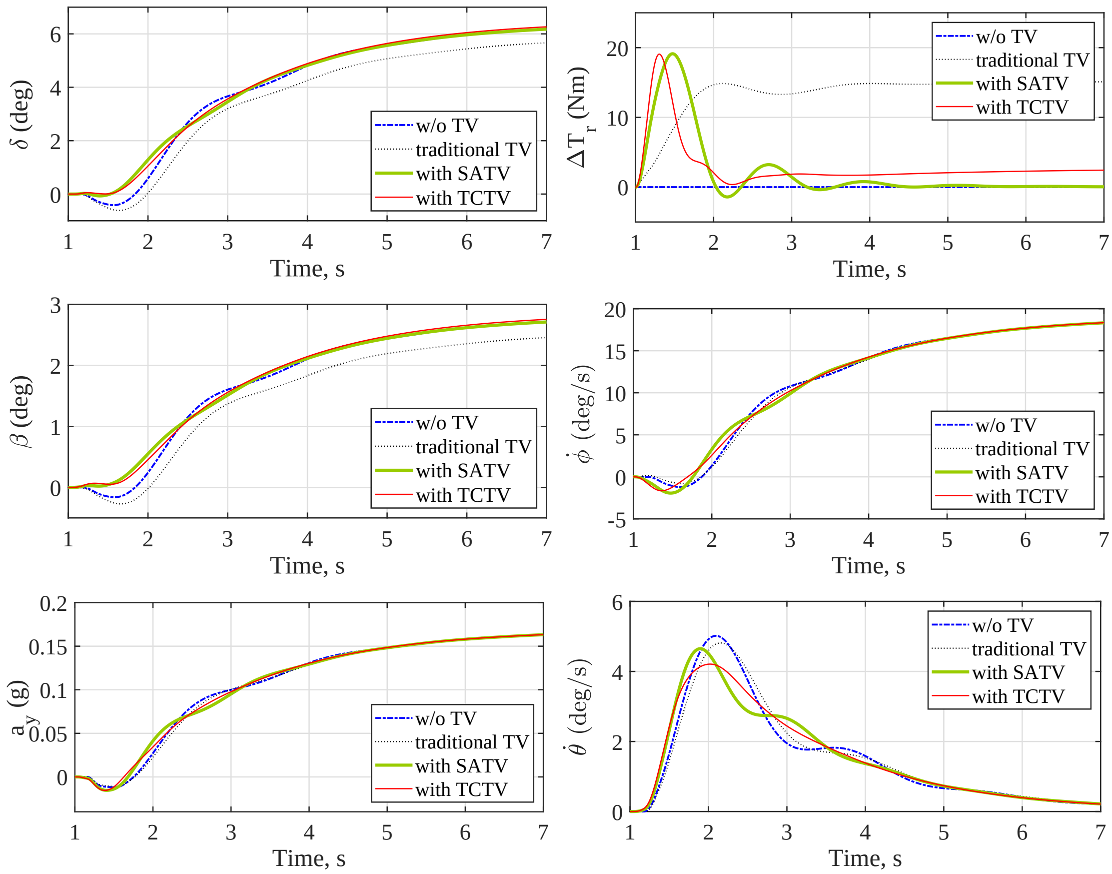


**Figure 10.** Simulation result of case 1 - left turn under constant speed.

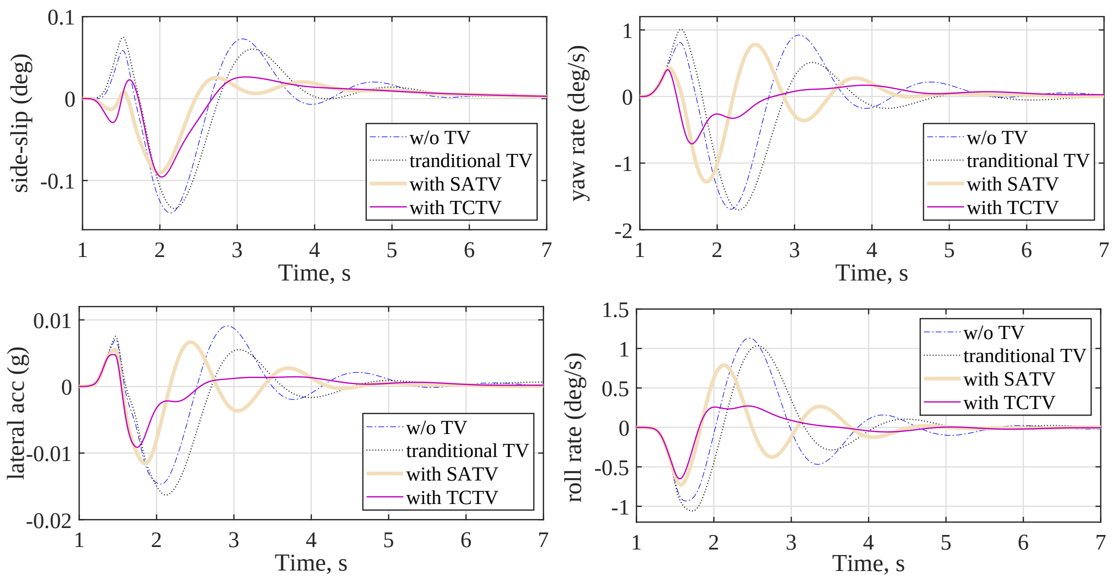


**Figure 11.** States tracking error comparison of case 1.

performance than the steering and torque control by rider but worse than that of the TCTV based torque control.

The states tracking error is shown in Figure 11 to get a more clear comparison. From the results of tracking error performance, the proposed controllers provided better performance in transient response with less oscillation rate and less maximum tracking error. In addition, the error has been eliminated to zero within about 4 seconds from the disturbance occurs. Thus, the proposed controllers achieve not only the stability of roll dynamic but also that of the steady-state as well.

The quantitative comparison result of maximum state tracking error and integral absolute error (IAE) is summarised in Table 3. The proposed TV control algorithm has less maximum error and oscillation comparing with the conventional rider controlled torque response and traditional TV approach. With the usage of TCTV, the counter steering from virtual rider is eliminated and the maximum error of

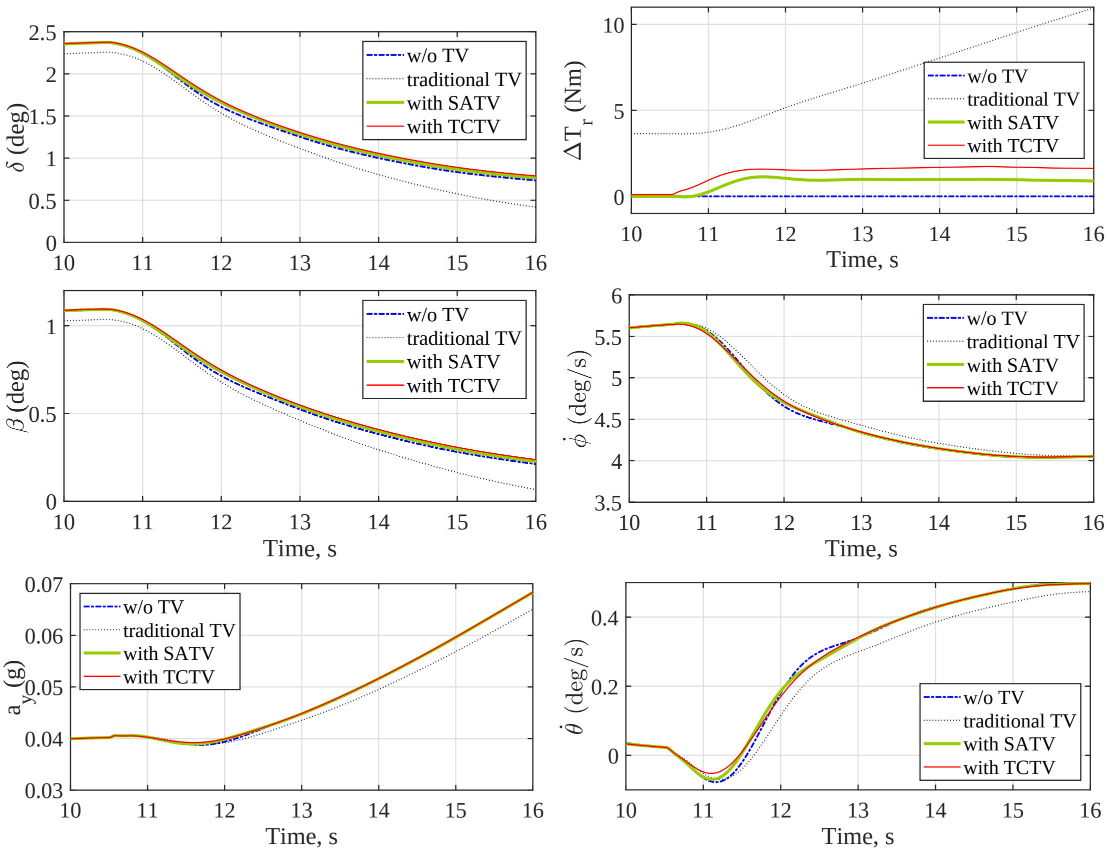


**Figure 12.** Simulation result of case 2 - acceleration during a turn.

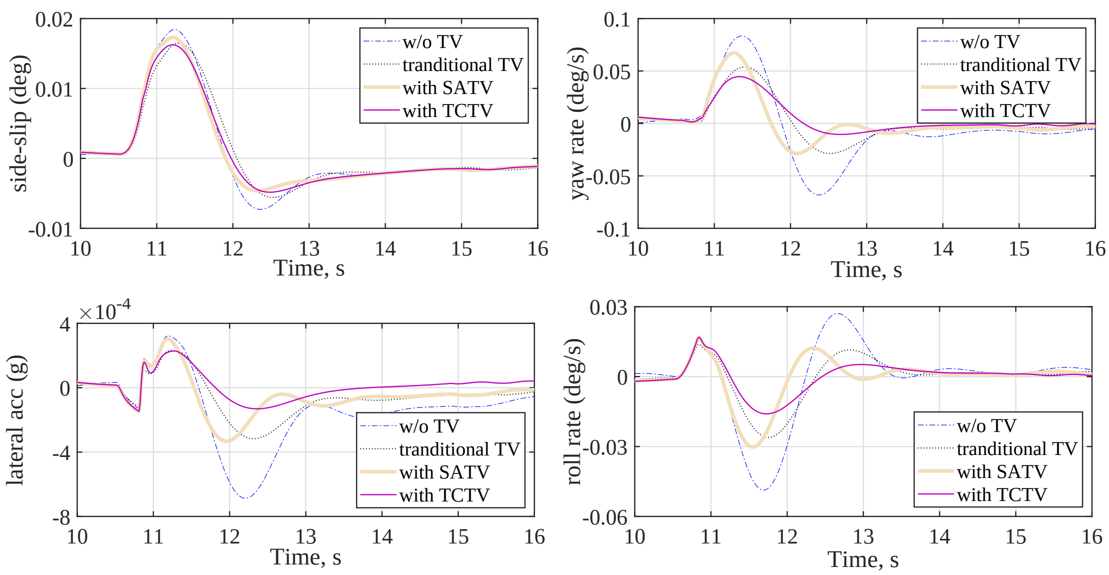


**Figure 13.** States tracking error comparison of case 2.

steering control is reduced about 74%. Other performance of the system dynamic response also have been improved because of the drive assistance by torque vectoring. The side-slip angle, yaw rate, lateral acceleration, and roll rate has 35%, 58%, 36%, 28% less maximum tracking error of steady state, respectively. To make the comparison more obvious to readers, the indices of the maximum error and IAE in percentages of their steady state value. Figure 14 shows the bar chart to compare the dynamic performance of system states.

### *Speed Acceleration during a Turn*

The constant speed turn of a NTV is much easier to balance the vehicle, while the speed change of both acceleration and deceleration will cause more instability of the vehicle especially the roll dynamics. The second case is designed under the condition of accelerating the speed of NTV during a turn. The initial state is the the vehicle is driven at the speed of a constant 5 $m/s$ and yaw rate of about 5.8 $deg/s$ in steady state. Then the rider increase the propulsion torque to accelerate the vehicle.

**Table 3.** Maximum state tracking error and integral absolute error comparison among different controllers of both cases

| Indices | Variables | Case 1: Drive into a turn with constant speed | | | | Case 2: Speed acceleration during a turn | | | |
|---|---|---|---|---|---|---|---|---|---|
| | | w/o TV | traditonal TV | with SATV | with TCTV | w/o TV | traditonal TV | with SATV | with TCTV |
| Maximum track error | Counter-steer agl (deg) | 0.553 | 0.311 | 0.107 | 0.006 | 0.053 | 0.013 | 0.0027 | 0 |
| | Side-slip agl (deg) | 0.1442 | 0.138 | 0.0943 | 0.101 | 0.0184 | 0.0165 | 0.0173 | 0.0162 |
| | Yaw rate (deg/s) | 1.763 | 1.82 | 1.307 | 0.719 | 0.0834 | 0.0539 | 0.0673 | 0.0447 |
| | Lateral acc ($\times 0.01$g) | 1.51 | 1.711 | 1.19 | 0.933 | 0.0687 | 0.0316 | 0.0332 | 0.0229 |
| | Roll rate (deg/s) | 1.166 | 1.086 | 0.803 | 0.653 | 0.049 | 0.0261 | 0.0302 | 0.0169 |
| Integral absolute error | Side-slip agl (deg) | 0.297 | 0.290 | 0.160 | 0.185 | 0.0266 | 0.0246 | 0.0242 | 0.0239 |
| | Yaw rate (deg/s) | 3.66 | 3.43 | 2.07 | 1.24 | 0.137 | 0.0793 | 0.0733 | 0.0535 |
| | Lateral acc ($\times 0.01$g) | 3.136 | 3.217 | 1.861 | 1.199 | 0.118 | 0.0619 | 0.0572 | 0.0367 |
| | Roll rate (deg/s) | 2.586 | 2.426 | 1.52 | 0.832 | 0.0628 | 0.0332 | 0.0263 | 0.0361 |

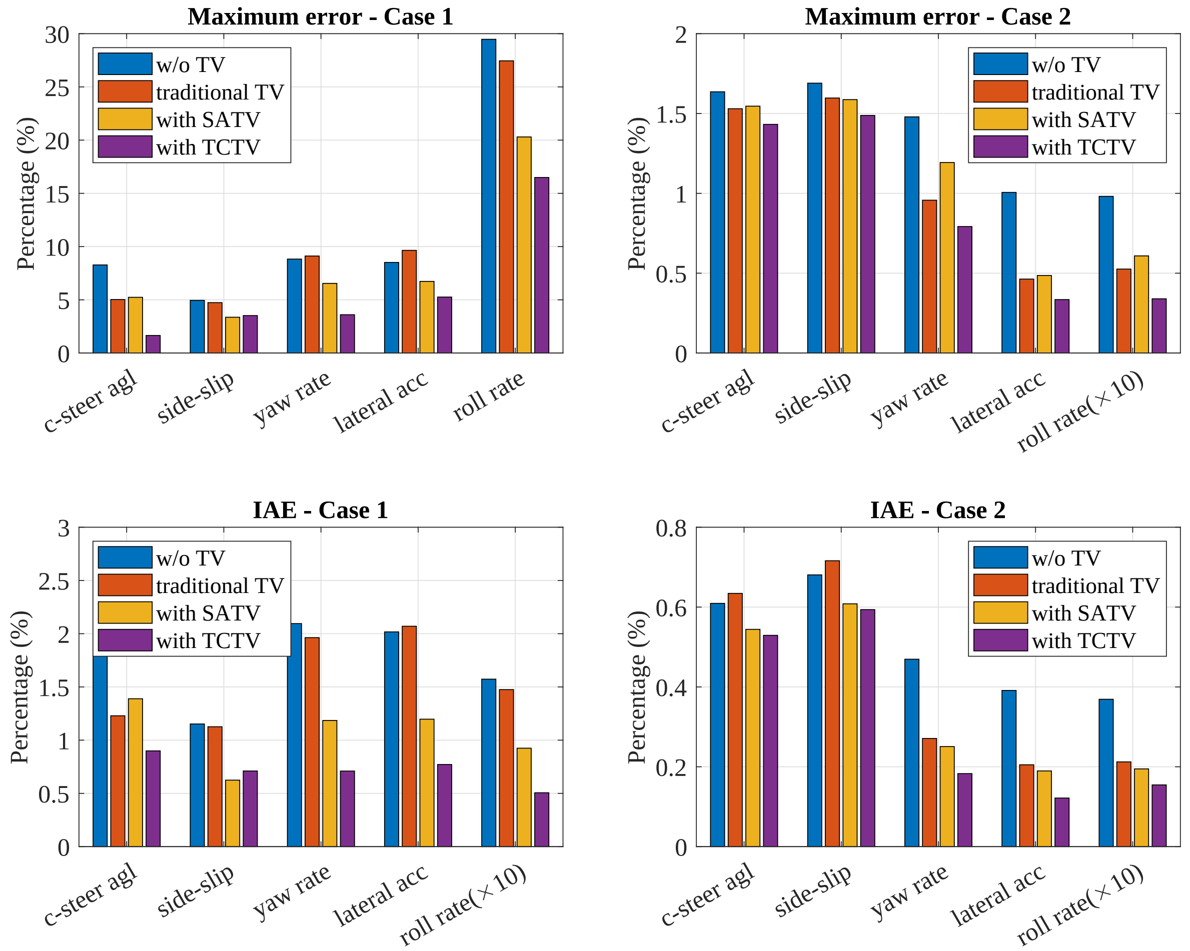


**Figure 14.** The performance indices comparison among different torque controllers.

Figure 12 shows the dynamic response of an NTV in this case, including two inputs and four system states. The states tracking error comparison is shown in Figure 13. Similar to the previous case, the SATV and TCTV based torque control have reduced the requirements of counter-steer from rider when accelerating in a turn. In the yaw rate and roll rate comparison, the TCTV performs the best with the least peak error and faster rising time. To make it more obvious to readers, the numerical results and bar chart comparison of maximum tracking error and IAE to steady state value have been given in Table 3 and Figure 14. The requirements of counter-steer has been fully eliminated from rider. The TCTV method has the ability to reduce the maximum error of steady state value in steer angle, side-slip, yaw rate, lateral acceleration and roll rate with 35%, 44%, 59%, 73% and 55%, respectively.

The cases aim to verify the control performance under a sudden disturbance on references in Case 1 and a time-varying disturbance on references in Case 2. The difference types of disturbance cause that the two cases achieved different performance in maximum error, oscillation rate and IAE value. From both cases, it can be concluded that, with the use of TV drive assistance method, the counter steering requirements can be fully eliminated from the rider, the maximum tracking error and oscillation rate of counter steer angle can be reduced for more than 1/3 of that without using torque vectoring. And the control performance of yaw rate, lateral acceleration and roll rate can be improved with a quarter to half reduction on the peak tracking error. Comparing the TCTV and the SATV methods, the tilting compensator eliminates the bad performance of maximum error and oscillation rate in SATV with further improvement in roll stability of NTV. The improvement is more obvious in a turn with speed acceleration, which has more challenges in balancing the vehicle. As the same rider model has been used in all tests, the NTV equipped with the torque vectoring based drive assistance system can help the rider, especially the new rider, to balance the vehicle during a turn under both a constant speed and an increasing speed. Therefore, the NTV equipped with the drive assistance system will be easy to be ridden by any types of rider with improved roll stability.

## Conclusion

This paper has designed two torque vectoring based drive assistance systems to help the rider in balancing the NTV during a turn and simplify the steering process. The two assistance systems, the steer angle based TV and the tilting compensator based TV, have been validated in simulation with the same rider model. From the simulation results, both TV based assistance methods eliminate the counter-steering requirements with improved roll stability in balancing the vehicle in the cases of constant speed turn and speed acceleration in a turn. In addition, with the tilting compensator, the unwanted maximum tracking error and oscillation rate of their steady state value have been reduced in all the dynamics of system states. The TCTV based drive assistance system can be used to help riders to balance the NTV in a turn without the dependency of riding experience from riders.

### Acknowledgements

The research presented in this article was undertaken as part of the Range of Electric Solutions for L Category Vehicles (RESOLVE) Project. Funded through the European Funding for Research and Innovation (Horizon 2020), Grant Number 653511.

### References

Ren Y, Dinh Q, Marco J, Greenwood D, and Hessar C. *Nonlinearity compentation based tilting controller for electric narrow tilting vehicles*. (2018), In 2018 5th International Conference on Control, Decision and Information Technologies (CoDIT), pages 1085–1090.

Ruggero F and Alessandro B (2006) *A virtual motorcycle driver for closed-loop simulation.* IEEE control systems, 26(5):62–77.

Fabien C, Ph C, and Lama M. *Non-linear control of a narrow tilting vehicle*. (2014), In 2014 IEEE International Conference on Systems, Man and Cybernetics (SMC), pages 2488–2494.

Dorina Pojani and Dominic Stead. *Sustainable urban transport in the developing world: beyond megacities*. (2015), Sustainability, 7(6):7784–7805.

Liang Li, Yishi Lu, Rongrong Wang, and Jie Chen. *A three-dimensional dynamics control framework of vehicle lateral stability and rollover prevention via active braking with MPC*. (2017), IEEE Transactions on Industrial Electronics, 64(4):3389–3401.

Auguste Van Poelgeest. *The Dynamics and Control of a Three-Wheeled Tilting Vehicle*. (2011), PhD thesis, University of Bath.

Joel Fajans. *Steering in bicycles and motorcycles*. (2000), American Journal of Physics, 68(7):654–659.

*RESOLVE project*.(2018), http://www.resolve-project.eu/.

Lama Mourad, Fabien Claveau, and Philippe Chevrel. *Direct and steering tilt robust control of narrow vehicles*. (2014), IEEE Transactions on Intelligent Transportation Systems, 15(3):1206–1215.

Antony Snell. *An active roll-moment control strategy for narrow tilting commuter vehicles*. (1998), Vehicle system dynamics, 29(5):277–307.

CR Van Den Brink and HM Kroonen. *DVC[1]-the banking technology driving the CARVER vehicle class*. (2004).

S Kidane, L Alexander, R Rajamani, P Starr, and M Donath. *A fundamental investigation of tilt control systems for narrow commuter vehicles*. (2008), Vehicle System Dynamics, 46(4):295–322.

Leonardo De Novellis, Aldo Sorniotti, and Patrick Gruber. *Wheel torque distribution criteria for electric vehicles with torque-vectoring differentials*. (2014), IEEE Transactions on Vehicular Technology, 63(4):1593–1602.

Kaoru Sawase and Yoshiaki Sano. *Application of active yaw control to vehicle dynamics by utilizing driving/breaking force*. (1999), JSAE review, 20(2):289–295, 1999.

Stefan Koehler, Alexander Viehl, Oliver Bringmann, and Wolfgang Rosenstiel. *Energy-efficiency optimization of torque vectoring control for battery electric vehicles*.(2017), IEEE Intelligent Transportation Systems Magazine, 9(3):59–74.

Kaoru Sawase, Yuichi Ushiroda, and Takami Miura. *Left-right torque vectoring technology as the core of super all wheel control (S-AWC)*. (2006) Mitsubishi Motors Technical Review, 18:16–23.

Kaoru Sawase and Yuichi Ushiroda. *Improvement of vehicle dynamics by right-and-left torque vectoring system in various drivetrains*.(2008), Mitsubishi Motors Technical Review, 20:14.

Juyong Kang, Hyundong Heo, et al. *Control allocation based optimal torque vectoring for 4WD electric vehicle*.(2012), Technical report, SAE Technical Paper.

Seongjin Yim, Jaewoong Choi, and Kyongsu Yi. *Coordinated control of hybrid 4WD vehicles for enhanced maneuverability and lateral stability*.(2012) IEEE Transactions on Vehicular Technology, 61(4):1946–1950.

Saber Fallah, Amir Khajepour, Barış Fidan, Shih-Ken Chen, and Bakhtiar Litkouhi. *Vehicle optimal torque vectoring using state-derivative feedback and linear matrix inequality*.(2013), IEEE Transactions on Vehicular Technology, 62(4):1540–1552.

Hyundong Her, Youngil Koh, Eunhyek Joa, Kyongsu Yi, and Kilsoo Kim. *An integrated control of differential braking, front/rear traction, and active roll moment for limit handling performance*.(2016), IEEE Transactions on Vehicular Technology, 65(6):4288–4300.

Pushpendra Kumar, Rochdi Merzouki, Blaise Conrard, Vincent Coelen, and Belkacem Ould Bouamama. *Multilevel modeling of the traffic dynamic*.(2014), IEEE Transactions on Intelligent Transportation Systems, 15(3):1066–1082.

Hans Pacejka. *Tire and vehicle dynamics*. (2005), Elsevier.

Jacob Svendenius. *Tire modeling and friction estimation*. (2007) PhD Theses.

S Kidane, L Alexander, R Rajamani, P Starr, and M Donath. *oad bank angle considerations in modeling and tilt stability controller design for narrow commuter vehicles*.(2006), In American Control Conference, 2006, pages 6

Samuel Kidane, Rajesh Rajamani, Lee Alexander, Patrick J Starr, and Max Donath. *Development and experimental evaluation of a tilt stability control system for narrow commuter vehicles*.(2010), IEEE Transactions on control systems technology, 18(6):1266–1279.

Dal Y Ohm. *Analysis of pid and pdf compensators for motion control systems*.(1994) In Industry Applications Society Annual Meeting, Conference Record of the 1994 IEEE, volume 2, pages 1923–1929.

J Gohl, Rajesh Rajamani, P Starr, and Lee Alexander. *Development of a novel tilt-controlled narrow commuter vehicle*. (2006).